

# ***A High-Power Magnetron Transmitter for Superconducting Intensity Frontier Linacs***

***G. Kazakevich, V. Yakovlev,  
R. Pasquinelli, B. Chase,  
G. Flanagan, F. Marhauser  
K. Quinn Jr. and D. Wolff***

## Requirements of the intensity-frontier GeV-scale superconducting proton or ion linacs to Continuous Wave (CW) RF sources:

- ▶ Powering Superconducting RF (SRF) cavities with deviations of the accelerating voltage in phase and amplitude of  $<1$  degree and  $<1\%$  of nominal, respectively.
- ▶ The average RF power to feed, for example, an ILC-type SRF cavity at the energy gain of  $\sim 20$  MeV/cavity and a 1-10 mA average beam current is a few tens to a few hundreds kW.
- ▶ Powering of each SRF cavity by an individual Low Level RF (LLRF) vector controlled RF source to prevent the beam emittance growth, [1], caused by mechanical oscillations in the SRF cavities, beam loading, dynamic cavity tuning errors, etc.

## Financial aspects for various RF sources intended for the intensity-frontier linacs:

- ▶ The investment costs for the RF power system for large-scale projects (e.g. ILC, Project-X, etc.) are a significant fraction of the overall costs if relying on traditional RF sources as klystrons, IOTs, or solid-state amplifiers.
- ▶ The CW magnetrons based on commercial prototypes are potentially less expensive than the above-listed RF sources, [2, 3], thus utilization of the magnetron RF sources in the large-scale accelerator projects will significantly reduce the capital cost; the CW magnetrons with power of tens to hundreds kW are well within current manufacturing capabilities.

▶ Operation of a magnetron injection-locked by a frequency (phase) modulated signal has been first demonstrated in simulation and measurements performed with a 2.5 MW 2.8 GHz pulsed magnetron type MI-456A locked by a signal with varying (slowly in the magnetron frequency domain) frequency, [4-6].

***The results demonstrated proof-of-principle of the frequency (phase) control of the injection-locked magnetron.***

▶ A transient process in the injection-locked magnetron caused by the modulated locking signal along with modulation of the magnetron current has been numerically simulated considering the magnetron as a forced (injection-locked) oscillator described by a derived abridged equation, [5].

▶ Measurements performed with a down-conversion techniques demonstrated very good agreement with the numerical simulation, [4-6]. The measurements verified operation of the magnetron in injection-locked mode at the control by the frequency (phase) modulated signal.

▶ Unlike the approach developed by R. Adler, [7], the technique simulating the transient process allows numerical computation of variations of the magnetron frequency (phase) in time domain, considering variations of the frequency (phase) of the locking signal and variation of the magnetron current.

► Further analysis [8], verified good linearity of the frequency and phase response of the injection-locked magnetron, Fig. 1, quite low phase distortion (with rms < 0.36 degrees) in the response at the frequency (phase) control, Fig. 2, and indicates a fairly wide bandwidth in the magnetron response.

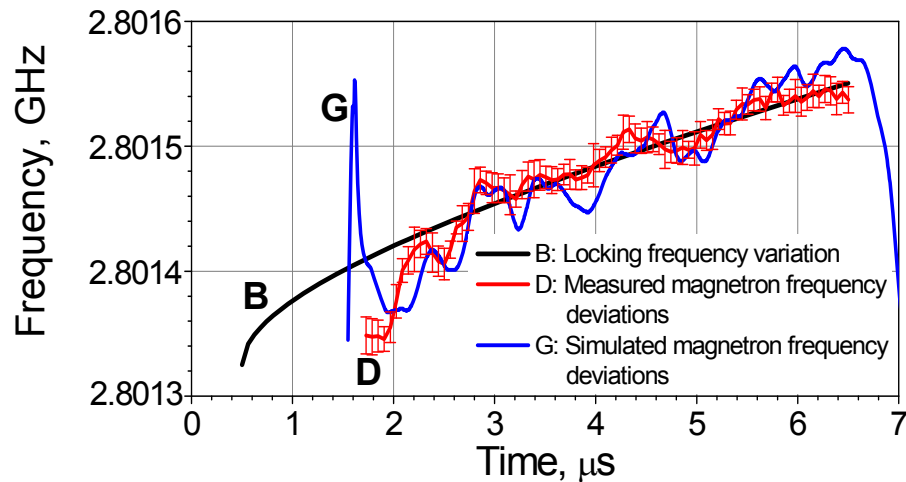


Fig. 1. Variation of the simulated (G), and measured magnetron frequency (D), vs. the locking frequency (B) variation.

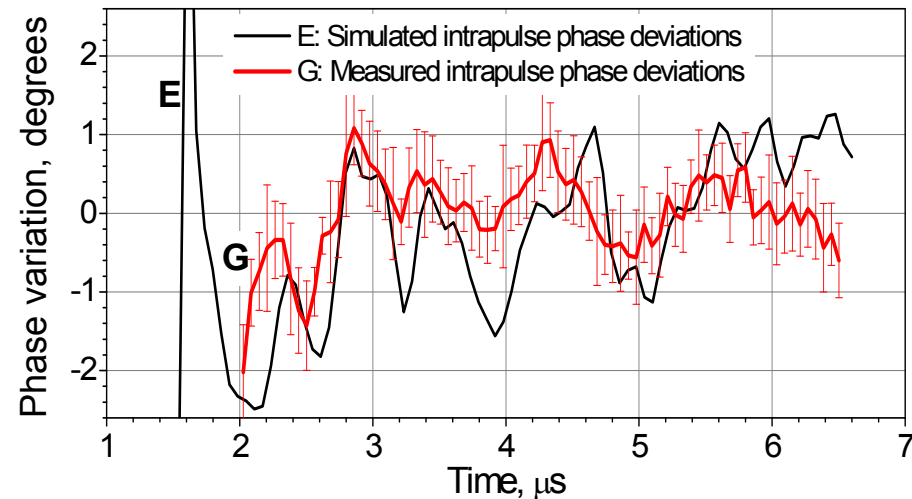


Fig. 2. Simulated, curve E, and measured, curve G, phase distortions in the magnetron response at the frequency/phase modulation.

***This formally allows consideration of the injection-locked magnetron as a linear (in limited range) device and substantiates operation of the injection-locked magnetrons with a phase control loop.***

Note that:

- ▶ *The transient process considered in [5, 6] quite well describes management of the injection-locked magnetron in frequency (phase) by the locking signal and/or by the magnetron current, describing the frequency (phase) pushing effect.*
- ▶ *To stabilize its phase, the injection (frequency)-locked magnetron can be managed by a closed loop controller. First it was demonstrated in experiments described in [2, 9, 10].*

# A CONCEPT OF THE MAGNETRON TRANSMITTER CONTROLLED IN PHASE AND POWER

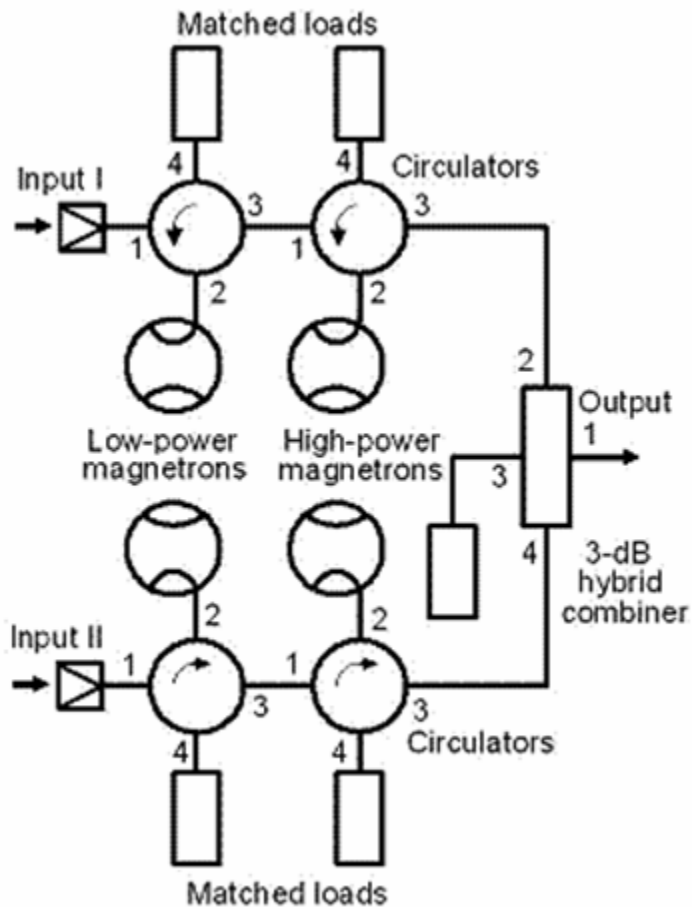


Fig. 3. Block diagram of the magnetron transmitter based on 2-cascade injection-locked magnetrons with a control in power and phase.

- ▶ The transmitter consists of two 2-cascade injection-locked magnetrons with outputs combined by a 3-dB hybrid, [11].
- ▶ The phase management is provided by a control of phase in both channels simultaneously, while the power management is provided by a control of phase difference on the inputs of the 2-cascade magnetrons.
- ▶ The 2-cascade injection-locked magnetron in which the low-power magnetron excites the high-power magnetron and all of tubes operate in injection-locked mode was proposed to decrease the locking power by -35 to -25 dB relatively to the combined output power.

# TECHNIQUES FOR EXPERIMENTAL TEST OF THE MAGNETRON TRANSMITTER CONCEPT

► All features of the transmitter were studied using two CW 2.45 GHz magnetrons with output power up to 1 kW. The magnetrons were chosen to be locked at the same frequency. The magnetrons were powered by a single pulsed modulator with partial discharge of storage capacitor of 200  $\mu\text{F}$ .

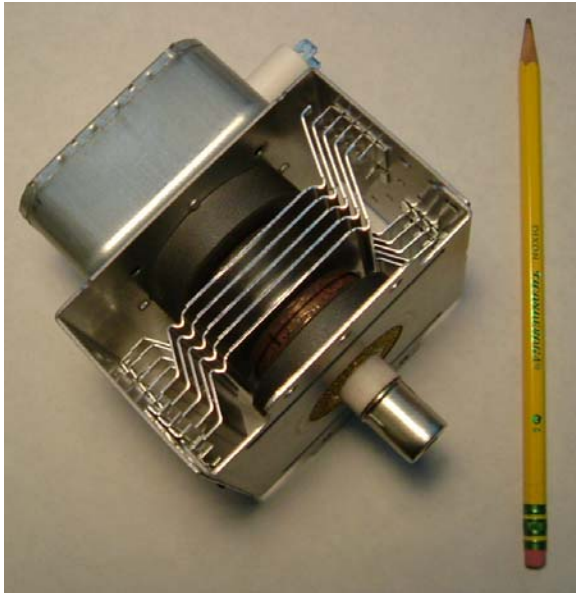


Fig. 4. Photo of the CW, 1 kW magnetron type 2M219J

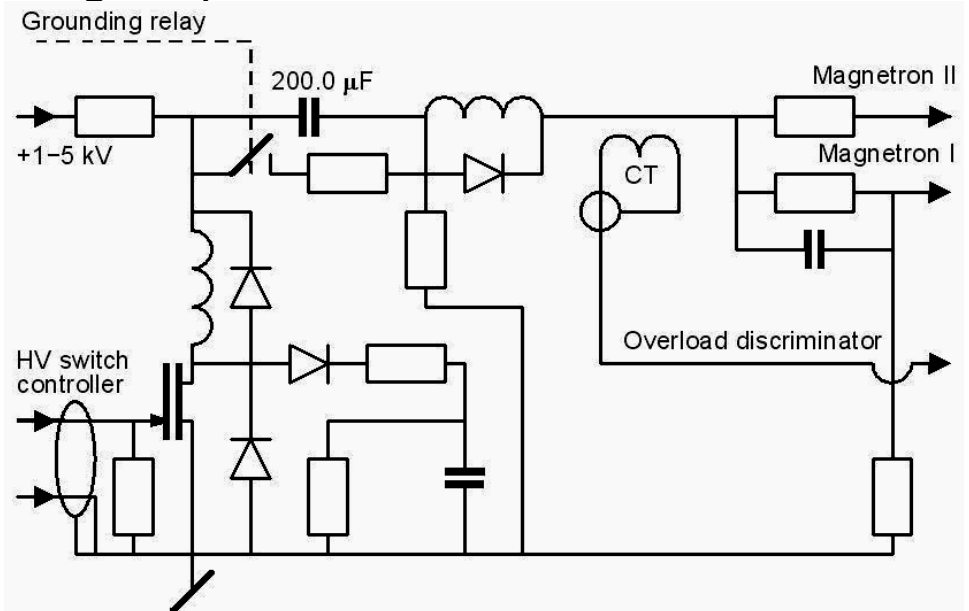


Fig. 5. Simplified scheme of the modulator HV module

► In simultaneous operation the lower voltage magnetron was powered from a compensated divider shown in Fig. 5.

► To protect the magnetrons and the modulator components from arcs the modulator has an interlock chain that rapidly interrupts the HV if the modulator load current exceeds 3.5 Amps.



Fig. 6. Photo of the modulator HV module

The modulator operating parameters:

Output voltage:	$U_{Out} = -(1-5) \text{ kV}$
Repetition rate:	0.25 Hz
Pulse duration:	2.5-15 ms
Output current:	$I_{Out} = 0.3-1.0 \text{ A}$

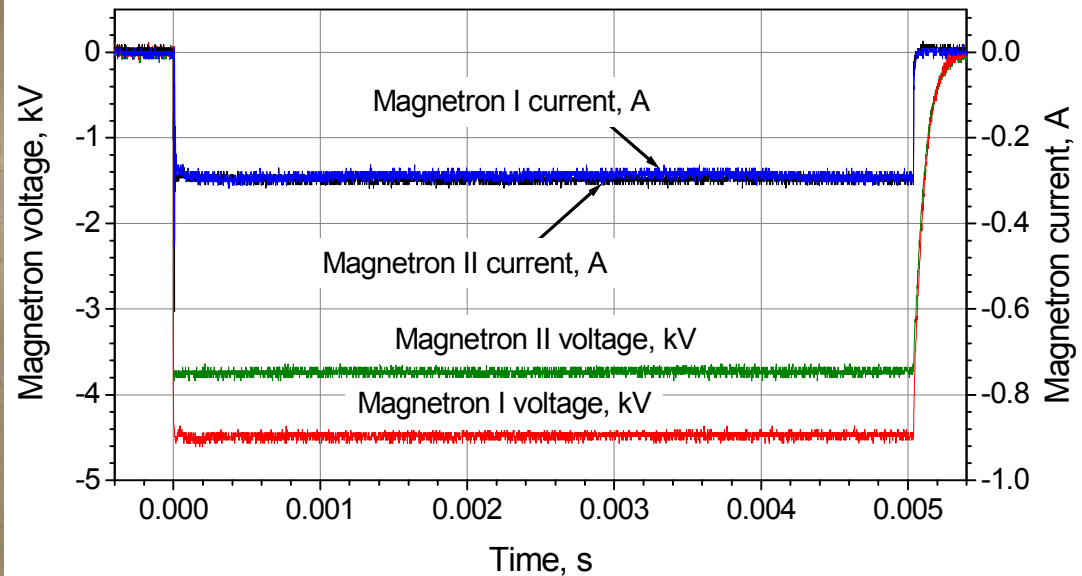


Fig. 7. Pulse shapes of voltages and currents of the magnetrons operating simultaneously

► Features of the transmitter based on injection-locked CW magnetrons have been studied using two modules with magnetrons 2M219J and OM75P(31), Figs. 8, 9.



Fig. 9. Photo of a module with a CW magnetron intended to work in injection-locked mode

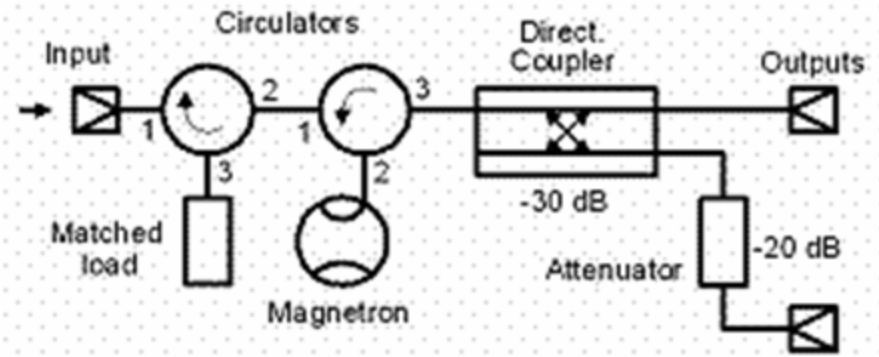


Fig. 8. The magnetron experimental module in which a CW magnetron operates as an injection-locked oscillator.

► The CW magnetrons were mounted on the WR430 waveguide sections coupled with a waveguide-coax adapters. The adapter and the section designs were optimized in 3-D by CST Microwave Studio to minimize reflection and maximize transmittance which are:  $S_{11} = -26.3$  dB and  $S_{21} = -0.1$  dB, respectively.

► The leakage field from the magnetron filament transformer was suppressed by a low-carbon steel screen not shown in Fig. 9.

► Verification of operation of the each CW magnetron in injection-locked mode was performed in pulsed regime while each magnetron was pre-excited by CW TWT amplifier driven by N5181A Agilent synthesizer as it is shown in Fig. 10, [8]. To measure intrapulse phase variations of the injection-locked magnetron, Fig. 11, a, b, the setup utilizes an interferometer including a trombone  $\phi$  (a phase shifter), a double balanced mixer, and a Low Pass Filter, LPF.

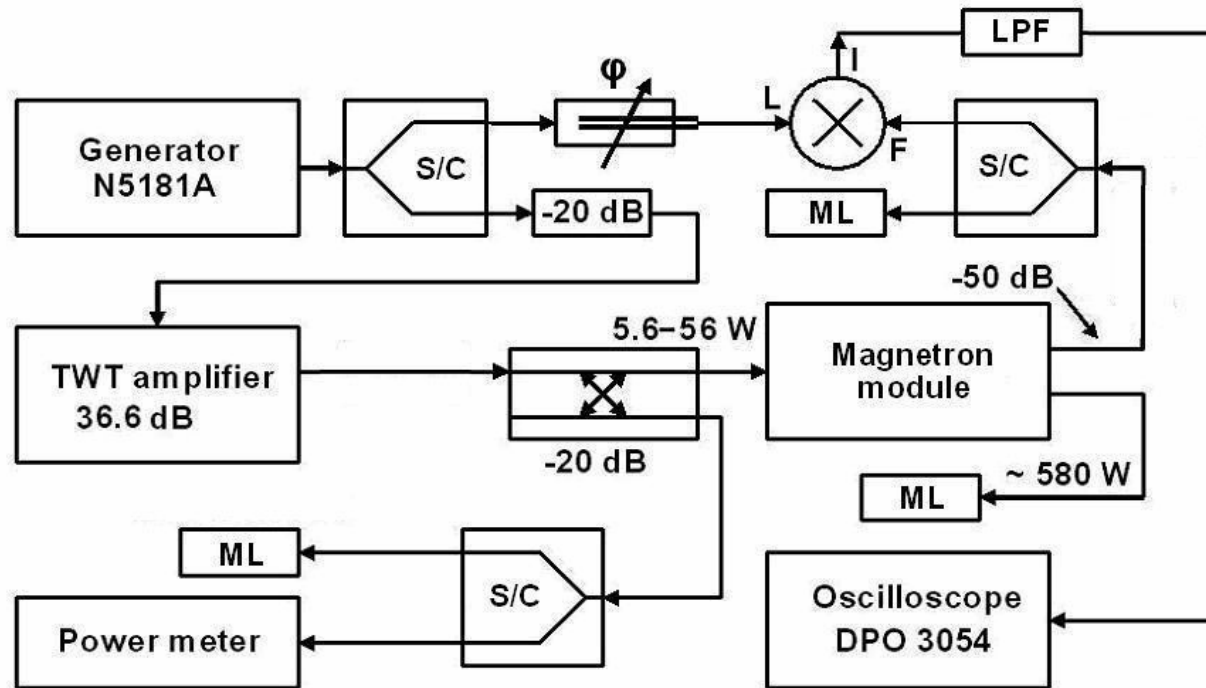
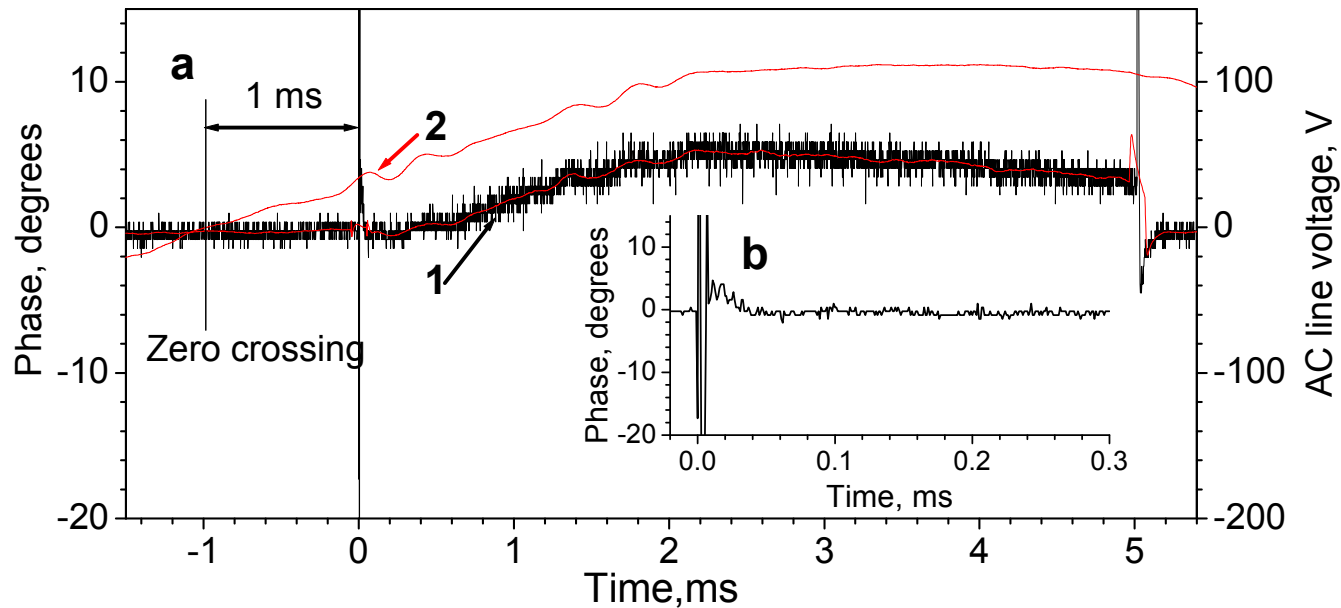


Fig. 10. Experimental setup with the interferometer to measure phase variations of the injection-locked magnetron. S/C is a 3-dB splitter/combiner; ML is a matched load.

► Traces in Fig. 11 show operation of magnetron in injection (frequency)-locked mode with phase variation  $\leq 5.3$  deg. (peak-to-peak) at pulse duration of 5 ms. Note that  $\sim 50$  deg. peak-to-peak phase variation with an injection-locked magnetron was measured in [2, 10], when the phase loop control was OFF.

► The measurements [2, 8, 10] demonstrated necessity in a Phase Locking Loop (PLL) control of the injection-locked magnetron if one needs a precise phase stability.



**FIG. 11. a. Phase variations of the injection-locked CW magnetron type 2M219J operating at pulse duration of 5 ms at  $P_{\text{Out}}/P_{\text{Lock}}=9.6$  dB, trace 1. Shape of the AC line voltage, trace 2. Inset b in the figure shows zoomed in time phase variation during first 0.3 ms.**

► Measured phase noise r.m.s. magnitude at  $t \geq 120 \mu\text{s}$  is  $\leq 0.6$  degrees.

- ▶ Notable phase variation on the leading edge of the modulator pulse during of  $\sim 50\text{-}100\ \mu\text{s}$ , Fig. 11b, may result from phase pushing caused by multipactoring in the magnetron cavity when the pulsed high voltage is applied or/and variation of emitting properties of the magnetron cathode caused by cleaning of the emitting surface by back-streaming electrons.
- ▶ Slow phase drift during the pulse one can explain by phase pushing resulted from competing processes: an increase of the magnetron current, most likely, because of overheating of the cathode surface caused by bombardment with back-streaming electrons and a decrease of the magnetron current associated with a drop of the magnetron voltage resulted from discharge of the modulator storage capacitor.
- ▶ Measured phase pushing resulted from the magnetron current variation is  $\sim 1.5\ \text{deg}/1\%$  or  $\sim 500\ \text{deg}/\text{A}$  at the ratio of the output power to the locking power of  $\sim 16\ \text{dB}$ .

► The alternative magnetic field induced by the magnetron filament circuitry also affects the phase instability of the injection-locked magnetron.

Phase distortions of the injection-locked magnetron synchronous with distortions of the network voltage are seen in Fig. 11a. The affect results are seen also in Fig. 12 showing dependence of the phase variation (peak-to-peak) vs. time shift,  $\Delta\tau$ , of the magnetron filament zero crossing relatively the modulator triggering.

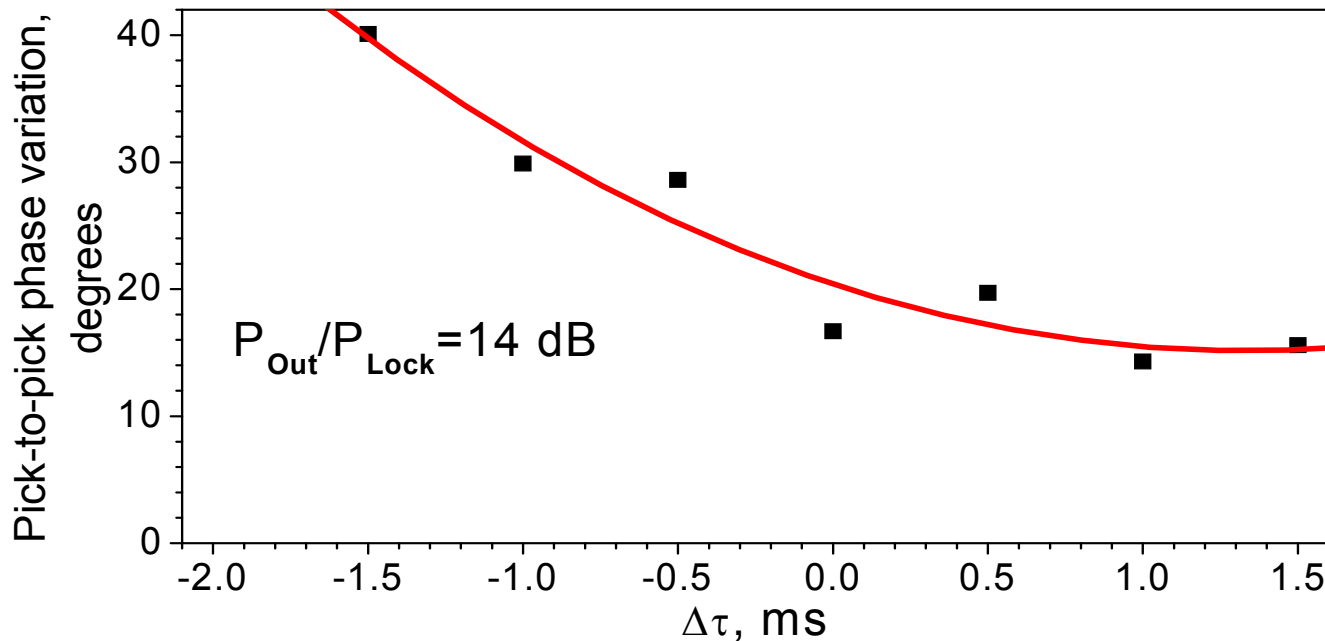
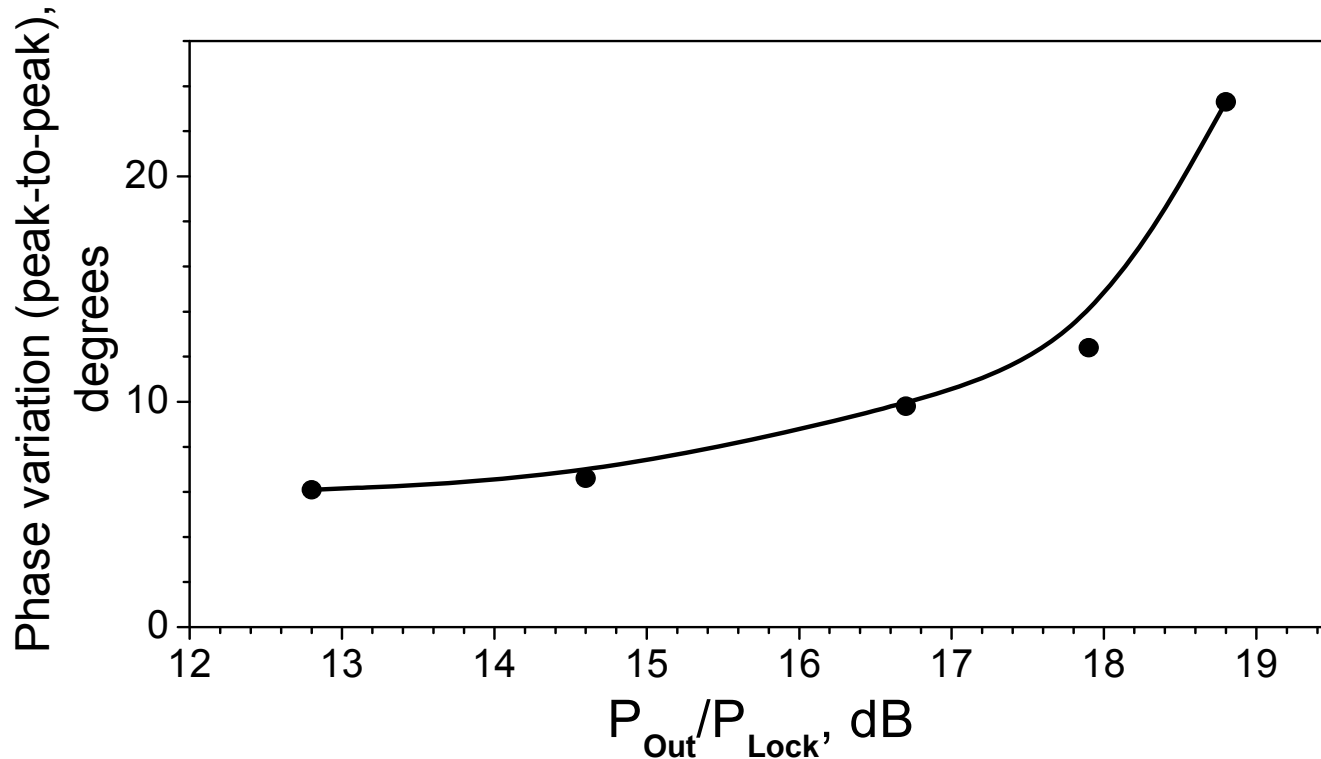


Fig. 12. Phase variation of the injection-locked magnetron vs. the time shift  $\Delta\tau$ .

▶ To minimize influence of the filament circuitry on the phase stability of the injection-locked magnetron we triggered modulator with time shift of 1 ms relatively the moment of the zero crossing of the magnetron filament current as it is shown in Fig 11a.

All measurements of the phase instability of the injection-locked magnetrons described in this work were performed with such modulator triggering.

► Measured peak-to peak phase variation of the injection-locked magnetron type 2M219J vs. the ratio of output power to locking power,  $P_{\text{Out}}/P_{\text{Lock}}$ , is shown in Fig. 13. The measurements were performed at the output power of  $505 \pm 5$  W.



**Fig. 13. Dependence of phase variation (peak to peak) of the injection-locked magnetron vs. the locking power measured at the output power of  $505 \pm 5$  W.**

# TEST OF CONCEPT OF THE 2-CASCADE MAGNETRON

► Operation of the 2-cascade injection-locked magnetron has been verified combining two magnetron modules in series through an attenuator to provide injection-locking in the second magnetron by lowered signal from the first injection-locked magnetron, [8], as it is shown in Fig. 14. Both of the injection-locked magnetrons were fed simultaneously by the pulse modulator at pulse duration of  $\approx 5$  ms.

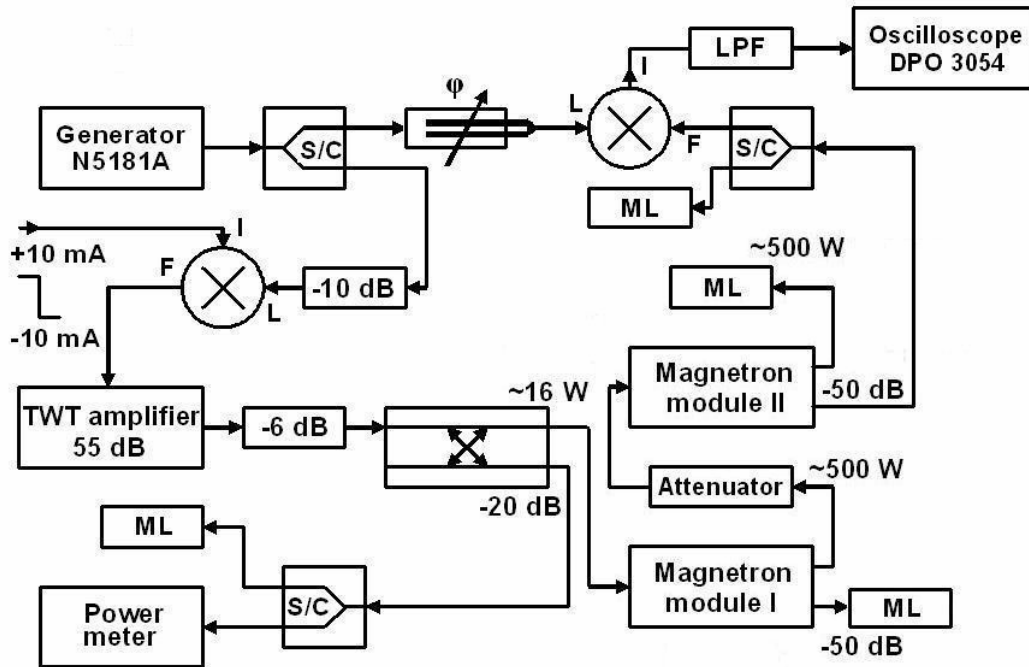


Fig. 14. Experimental setup to measure phase variation of the 2-cascade injection-locked magnetron

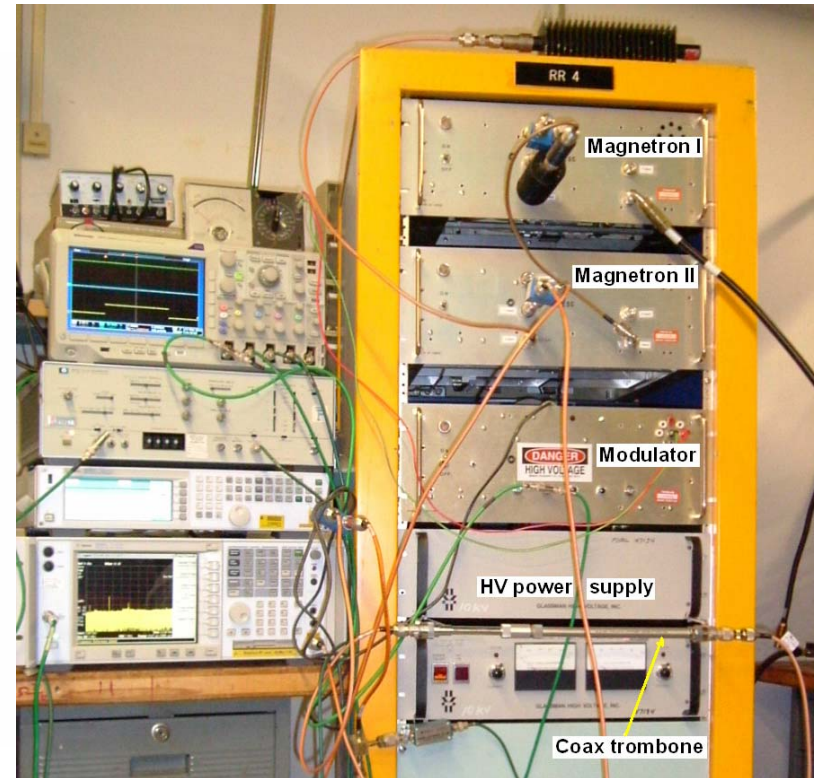


Fig. 15. Experimental setup to study 2-cascade injection-locked magnetron

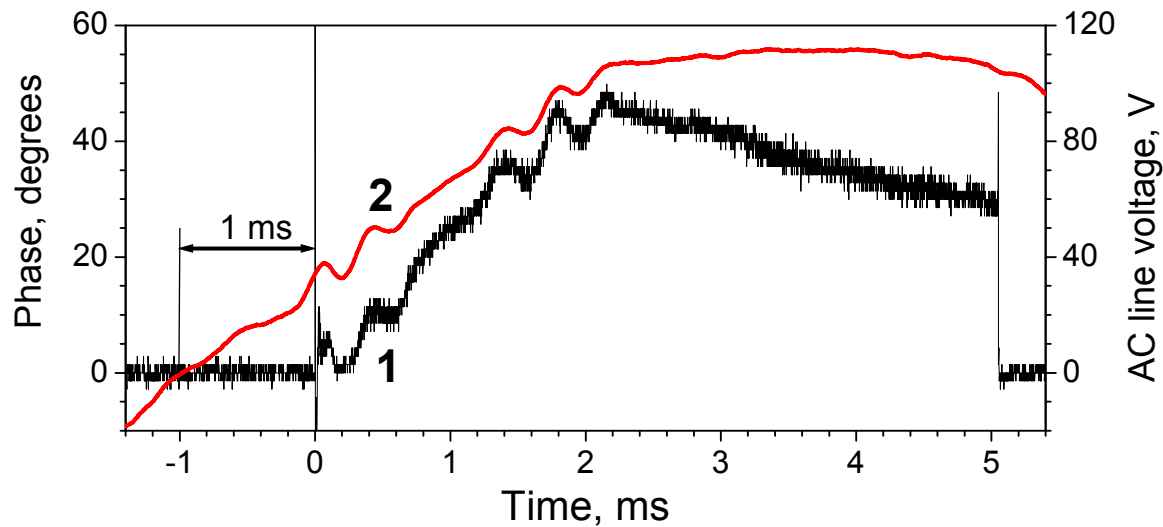


Fig. 16. Phase variations of the 2-cascade injection-locked magnetron measured for pulse duration of  $\approx 5$  ms at the attenuator value of 15 dB, trace 1; shape of the AC line voltage, trace 2.

***Experimental model of the 2-cascade magnetron demonstrated operation in injection-locked mode at ratio of the output power to the locking power of  $\sim 30$  dB considering the attenuator value.***

- ▶ The measured trace of phase variation of the 2-cascade injection-locked magnetron resembles the trace of the injection-locked single magnetrons, but magnitudes of the phase variation and phase distortions caused by induced magnetic field are larger.
- ▶ Measured noise r.m.s. magnitude at  $t \geq 120 \mu\text{s}$  is  $\leq 1.2$  degrees at the measured ratios of the output power to the locking power and at the output power of  $\approx 500$  W.

► The phase response of the 2-cascade injection-locked magnetron model on the fast 180 degrees phase flip has been roughly estimated using setup shown in Fig. 14, [12]. The 180 degrees phase flip in the TWT drive signal is accomplished, Fig. 17, with a pulse generator and double balanced mixer on the TWT amplifier input.

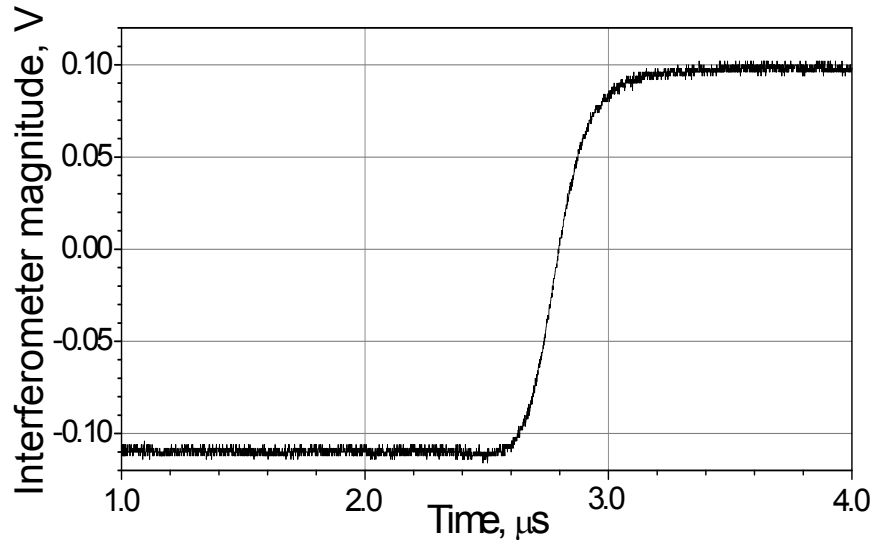


Fig. 17. Response of the frequency-locked 2-cascade magnetron on a fast 180 degrees phase flip measured at ratio of the output power to locking power of 26.5 dB; the interferometer calibration is  $\sim 0.8$  degrees/mV.

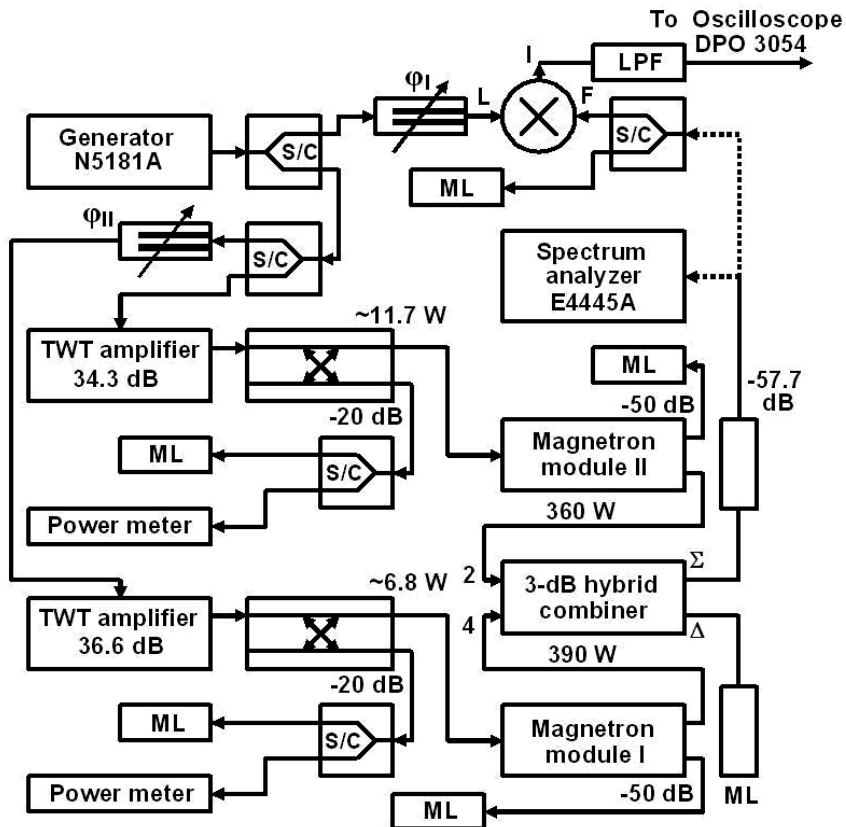
► The transient process of the 180 degrees phase flip response, Fig. 17, takes  $\sim 300$  ns.

► The plot demonstrates fast response of the 2-cascade injection-locked magnetron on a large like step-function variation of the controlling phase. This indicates a quite wide bandwidth in the phase control of the 2-cascade magnetron.

***The traces in Figs. 16, 17 demonstrate capability of the 2-cascade injection-locked magnetrons for a rapid phase control.***

# EXPERIMENTAL VERIFICATION OF THE POWER CONTROL CONCEPT IN THE PROPOSED TRANSMITTER

► A setup to study the power control of the injection-locked CW 2.45 GHz low-power magnetrons with 3-dB 180 degrees hybrid combiner is shown in Fig. 18.



► A phase shifter (trombone)  $\phi_{II}$  is used to vary the power combined on port " $\Sigma$ " of the 3-dB 180 degrees hybrid by variation of the phase difference in RF signals locking the magnetrons; the spectrum analyser E4445A is used to measure the combined power.

► The interferometer with the phase shifter  $\phi_I$ , double balanced mixer and LPF was used to measure phase deviations in the power controlled scheme.

► Measured power levels shown in Fig. 18 correspond to ratios of the output power to the locking power of 17.6 dB and 14.9 dB, respectively.

Fig. 18. A setup for test of the power control concept using the CW, 2.45 GHz, 1 kW injection-locked magnetrons with power combining.

03/26/2013

G. Kazakevich et al.,  
grigory@muonsinc.com

20

► Results of the power combining vs. the phase difference caused by variation of the phase shift  $\varphi_{II}$  by the trombone  $\varphi_{II}$  are plotted in Fig. 19 showing measured power on the combiner outputs “ $\Sigma$ ”, curve B, and “ $\Delta$ ”, curve C, considering the hybrid insertion losses of 0.4 dB and 0.7 dB, respectively. Curve E shows fit of the curve B by a  $\sin(\varphi_{II})$  function.

**Good agreement of the measured combined power, curve B, with the fit trace, curve E, verifies that the proposed concept of power control does not disturb operation of magnetrons in the injection-locked mode and demonstrates proof-of-principle of the proposed concept of power control in the transmitter based on injection-locked magnetrons with power combining.**

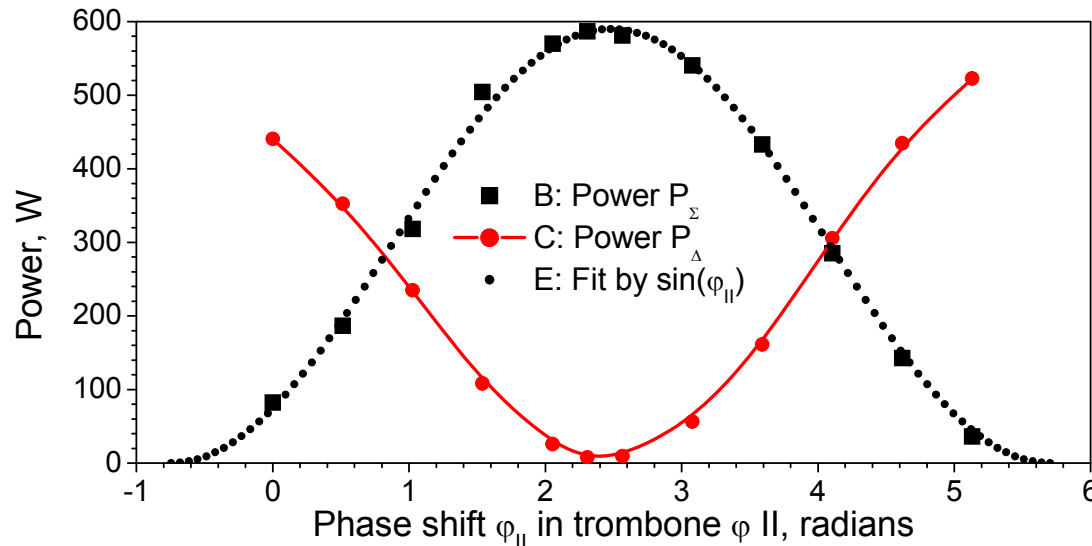


Fig. 19. Control of combined power by the phase difference in the injection-locked magnetrons.

► Phase variation of the injection-locked magnetrons with the power combining has been measured using setup shown in Fig. 18. At the measurements the trombone  $\varphi$  II length has been chosen to provide maximum signal on the hybrid port “ $\Sigma$ ”. Part of the trace measured with calibrated interferometer, Fig. 20, at  $t \geq 120 \mu\text{s}$  has a smooth shape with phase noise rms amplitude of  $\leq 1.3$  degrees.

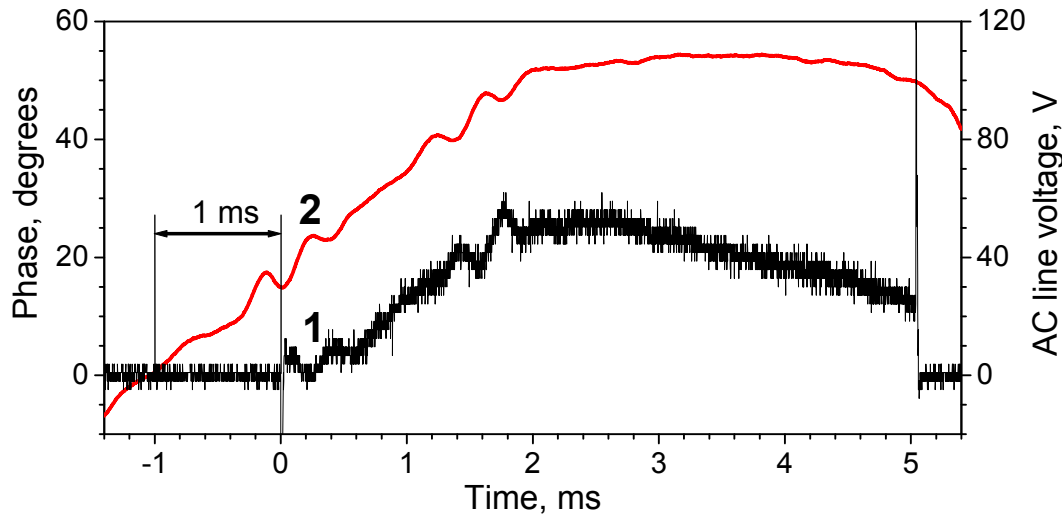


Fig. 20. 1- the interferometer trace at the output “ $\Sigma$ ” of the hybrid, 2- shape of the AC line voltage.

locked magnetrons because of larger discharge of the modulator storage capacitor loaded by two magnetrons.

► The phase trace resembles the traces of single magnetrons or 2-cascade magnetron. The phase variation magnitude (peak-to-peak) is  $\approx$  sum of magnitudes of the phase variations of the combined magnetrons. Larger phase variation at  $t \geq 2.5$  ms for magnetrons with power combining in comparison with a single magnetron results from larger phase pushing in the injection-

**Smooth shape of the phase variations of the combined in power magnetrons at  $t \geq 120 \mu\text{s}$  demonstrate that the magnetrons operate in injection-locked mode.**

▶ Demonstrated above linearity of the frequency (phase) response, Fig. 1, and low instantaneous phase noise of the injection-locked magnetrons (which are forced oscillators) allows formal consideration of the magnetrons as linear devices described by transfer characteristics of a transfer function to model a closed loop control.

▶ The bandwidth of the phase management of the injection-locked magnetrons necessary for the modelling was determined by measurements of the magnitude transfer characteristics of the phase control of the magnetrons with setups shown in figures 10 and 14 using phase modulation with low magnitude (0.07 rad.  $\approx$  4 degrees) in the synthesizer. The transfer characteristics have been measured by the Agilent MXA N9020A Signal Analyzer in the phase modulation domain mode. Non-flatness of the synthesizer phase characteristic has been measured and taken into account.

Transfer magnitude characteristics (rms values) of the injection-locked single 2M219J magnetron and the 2-cascade magnetron model averaged over 8 pulses are plotted vs. ratios  $P_{\text{Out}}/P_{\text{Lock}}$  in Fig. 21.

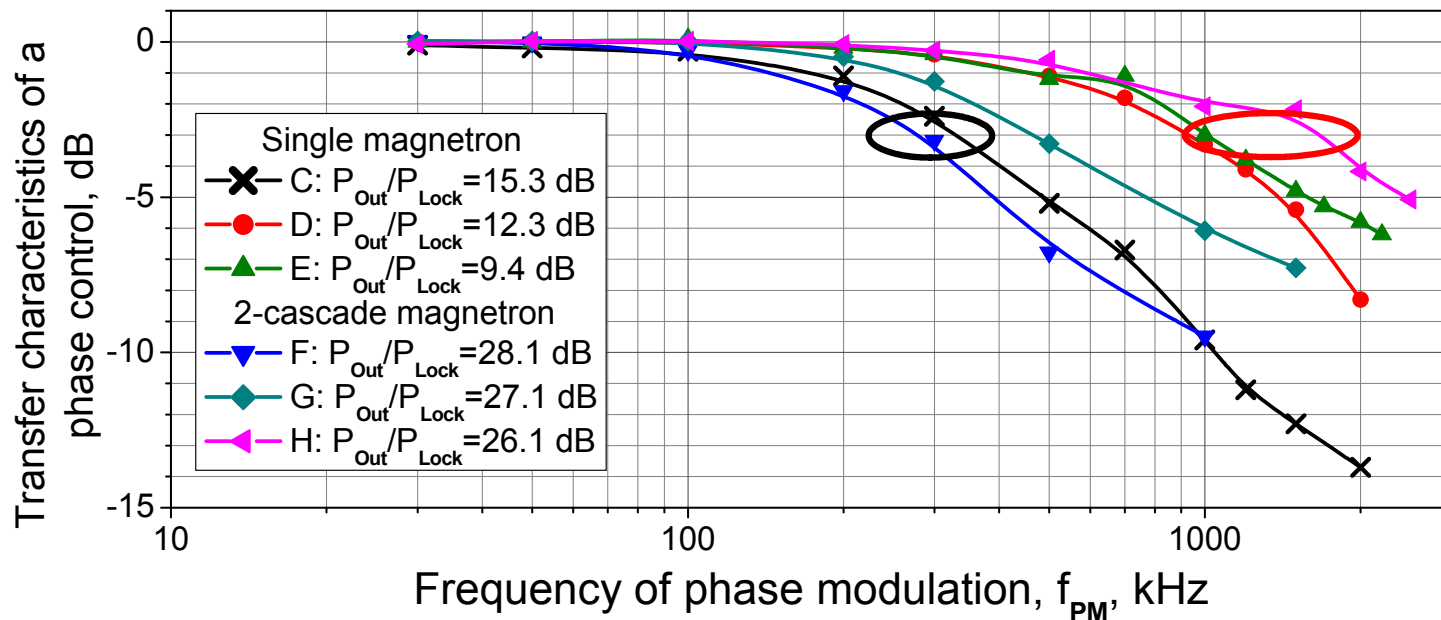


**Fig. 21. Transfer functions (rms values) of the phase control measured in phase modulation domain with single and 2-cascade injection-locked magnetrons for various ratios  $P_{\text{Out}}/P_{\text{Lock}}$  measured at  $P_{\text{Out}} \approx 450$  W.**

- ▶ The measured transfer characteristics of the phase control of the magnetrons demonstrate wide bandwidth, that allows the fast phase control of the magnetrons.
- ▶ The measured cutoff frequency of the phase modulation controlling the injection-locked magnetrons depends on ratio of the magnetron output power to power of the locking signal.
- ▶ The cutoff frequency of the phase modulation is  $\approx 300$  kHz at the locking power relative to the output power (per magnetron in the 2-cascade scheme) about of -14 dB or less, while at the locking power relative to the output power (per magnetron in the 2-cascade scheme)  $> -13$  dB the cutoff frequency of the phase modulation is  $\geq 1.0$  MHz.

- ▶ The transfer characteristics of the phase control in the phase modulation domain, Fig. 21, implies that a Low Level RF controller may have a closed loop with a bandwidth of  $\geq 100$  kHz and will be able to suppress all expected system disturbances like the parasitic frequency/phase modulation with the frequency about of hundreds Hz including phase disturbances from SRF cavity beam loading and the cavity dynamic tuning errors.
- ▶ For a phase locking loop with integral gain  $I=1.2 \cdot 10^7$  rad./s the parasitic modulation caused by HV power supply ripples at frequency  $f_r=120$  Hz will be suppressed by  $\approx 20 \log(I/2\pi f_r) \approx 84$  dB.

► Influence of the phase noise of injection-locked magnetrons on the accelerating field in the SRF cavity has been numerically simulated with a simple model of a proportional-integral (PI) feedback phase loop around a superconducting cavity with a broad-band disturbance, Fig. 22. A 200 Hz half bandwidth low-pass filter models the cavity base-band response, a 400 kHz bandwidth noise source represents the phase noise of the magnetron and a 2  $\mu$ s delay represents all system group delay. The PI loop is setup with a proportional gain of 200 and integral gain  $I=1.2 \cdot 10^7$  rad./s.

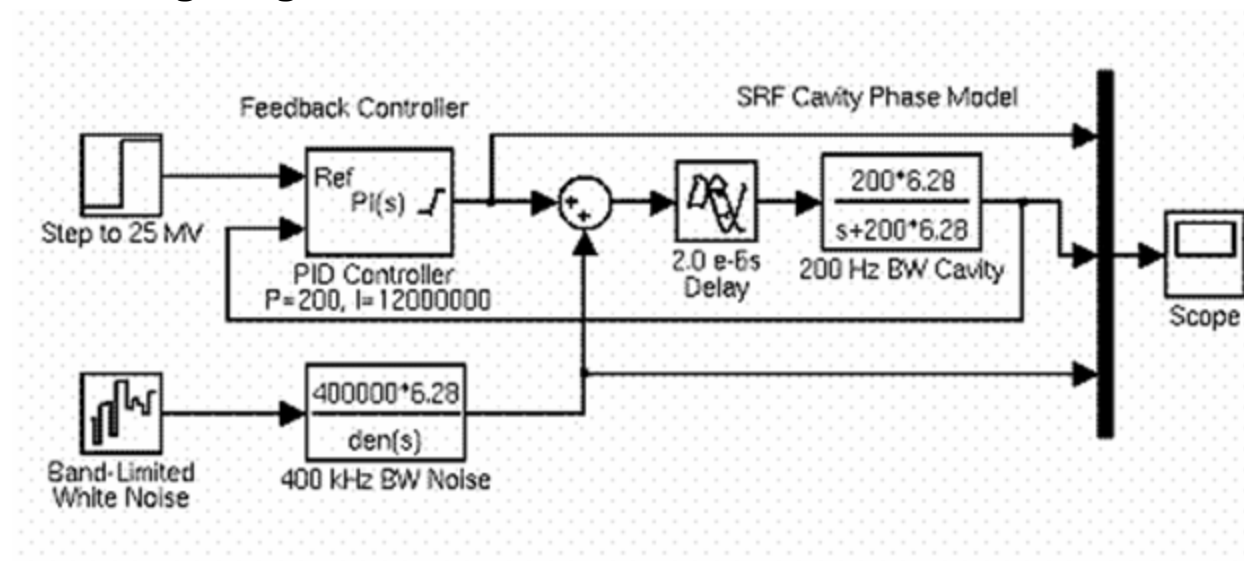


Fig. 22. Simplified model of a LLRF system controlling a superconducting cavity. The loop proportional gain is 200, the integral gain is  $1.2 \cdot 10^7$  rad./s, the group delay is 2  $\mu$ s.

► The performed numerical modelling, Fig. 23, demonstrate that the broad band noise associated with the greatly exaggerated magnetron noise is suppressed by the controller with the PI loop including the SRF cavity by  $\approx 50$  dB for peak-to-peak measurements.

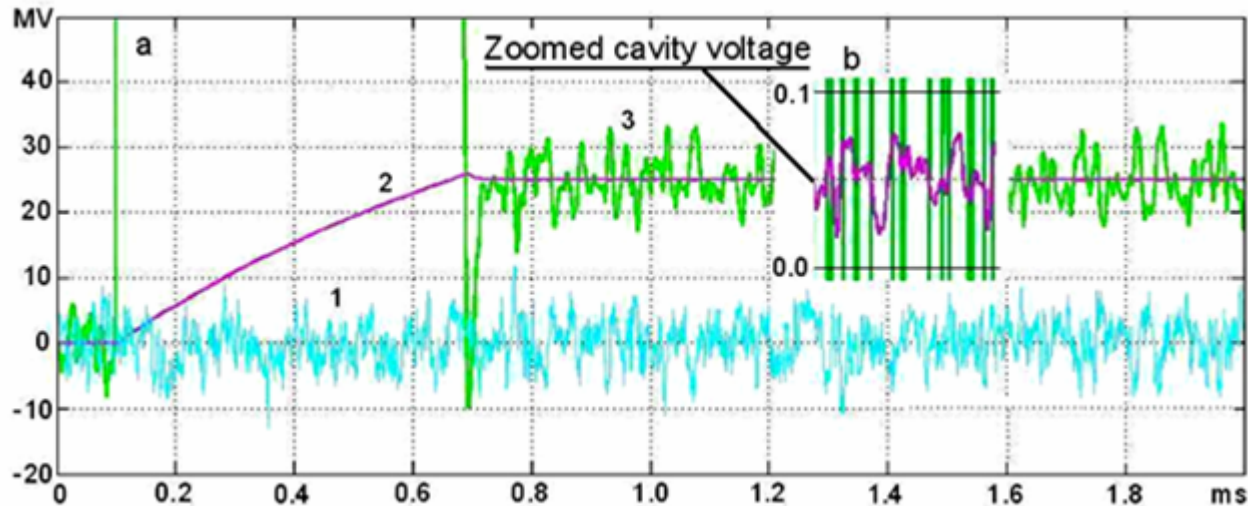


Fig. 23. Traces shown in figure “a” are: curve 1 is the 400 kHz bandwidth disturbance, curve 2 is cavity voltage, curve 3 is RF drive. Vertical scale is 10 MV/division. The inset “b” presents zoomed in  $\approx 300$  times (in vertical) trace of the cavity voltage, curve 2, in time domain. Vertical scale in the inset “b” is 0.1 MV/division.

► Since measured instantaneous phase noise amplitude for the injection-locked magnetrons is  $\leq 1.3$  degrees one expects that the accelerating field amplitude instability caused by the magnetron instantaneous phase noise will not exceed 0.01%.

## **SUMMARY**

*The presented work demonstrates quite low phase noise of the injection-locked magnetrons and acceptable linearity in response on the phase control. Measured magnitude characteristic of the magnetron transfer function at the phase modulation control demonstrates quite wide bandwidth of the magnetron response. This allows consideration of the injection-locked magnetrons as linear devices at the phase control and substantiates operation of the injection-locked magnetrons with phase control loop. Modeling of the closed control loops with wide bandwidth demonstrates suppressing of any relatively low-frequency parasitic modulation in SRF cavities driven by the RF sources based on the phase-controlled injection-locked magnetrons.*

- ▶ *Measurements of the transfer characteristic of the phase control with the CW injection-locked magnetrons demonstrated wide bandwidth acceptable for the phase control loop with bandwidth of  $\geq 100$  kHz for all active components of the proposed transmitter including the 2-cascade magnetrons.*
- ▶ *Evaluation of parasitic modulation caused by mechanical noises (microphonics and Lorentz-force noises) in the SRF cavity included in the appropriate phase control loop demonstrates that the modulation will be suppressed by  $\sim 80$  dB or more.*
- ▶ *Numerical modelling of operation of the SRF cavity powered by the injection-locked magnetron transmitter demonstrates that amplitude instability of the accelerating voltage resulted from the magnetron instantaneous phase noise will not exceed 0.01%.*
- ▶ *Proof-of-principle of the concept of proposed magnetron transmitter based on CW injection-locked 2-cascade magnetrons with a fast control in phase and power has been demonstrated in the experiments and numerical modelling.*
- ▶ *We plan to continue our efforts in experiments with dynamic control of the transmitter's phase and power.*

# REFERENCES

- [1] N. Solyak et al., LINAC10 Proceed., 2010.
- [2] A.C. Dexter et al., PRST-AB, 14, 032001, 2011.
- [3] R. Pasquinelli, "RF Power sources for Project X",  
<https://indico.fnal.gov/contributionDisplay.py?sessionId=4&contribId=12&confId=6098>.
- [4] G. Kazakevitch et al., NIM A 528, (2004), 115.
- [5] G. Kazakevich et al., PRST-AB, 12, 040701, 2009.
- [6] G. Kazakevich et al., NIM A 647, 10-16, 2011.
- [7] R. Adler, "A study of locking phenomena in oscillators," Proceedings of the I.R.E. and Waves and Electrons, 34: 351-357, June 1946.
- [8] G. Kazakevich et al., WEPPC059, IPAC12, Proceed., 2012.
- [9] I. Tahir et al., IEEE Transactions on Electron Devices, V 52, No 9, 2096-2103, 2005.
- [10] H. Wang et al., IPAC10 Proceed., 2010.
- [11] G. Kazakevich, V. Yakovlev, "Magnatron option for a pulse linac of the Project X" Project X document 896, <http://projectx-docdb.fnal.gov>
- [12] G. Kazakevich et al., WEPPC060, IPAC12 Proceed., 2012.

Thanks a lot to Dr. R. Johnson, Dr. S. Holmes,  
Dr. S. Henderson, Dr. V. Lebedev, Dr. S. Nagaitsev,  
Dr. R. Kephard, Dr. J. Raid, Dr. N. Solyak,  
Prof. O. Nezhevenko  
for permanent interest and strong support!

Thanks a lot to our friends and colleagues for  
kind help and support!

Thank you!